Determination of representative crack density of cementitious materials

H. H. Pan, Y. W. Chen & D. H. Lin
Dept. of Civil Engineering, Kaohsiung University of Applied Sciences, Kaohsiung, Taiwan

ABSTRACT: Based on the micromechanics approach and SEM measurements, a representative crack density parameter is chosen to evaluate elastic moduli and the stress intensity factor of high-performance concrete. Following the predicted material properties containing no cracks, one can estimate the effective material properties if their crack densities are given. SEM specimens were taken in the middle part of high-performance concrete, and each sample was observed at the fixed and random position to measure the micro-cracks with five magnifications from 500× to 5000×. The micromechanics-based calculations were compared with the experimental data to verify the reliability of representative crack density parameter. It is found that the optimum SEM magnifications for the representative crack density parameter of cementitious materials are of 3000× ~ 5000×, especially the magnification near 3000× is suitable for HPC containing $c_1 = 0.67$.

1 INTRODUCTION

The crack density calculation of cementitous materials depends on the number, the length, the width, the arrangement and the distribution of the cracks inside the material, and the observation methods. For a scanning electron microscope (SEM), for example, different observation magnifications of the specimen will result in different measurements of the cracks. Although many theoretical and experimental methods have been proposed to estimate and measure the crack density for brittle solids (Attiogbe & Darwin 1986, Attiogbe & Darwin 1987, Erick 1988, Oillivier 1985), it is still difficult to know the true crack density of cement-matrix composites up to now.

In this paper, one tries to find a representative crack density parameter (RCDP) of cementitous materials depending on the SEM magnifications, and this RCDP will be examined by the micromechanics theory and the experiments to confirm the reliability in use. Two SEM observations were chosen to view the microcracks: fixed position and random position, where the fixed view means that the inspection position of the cracks always locates in the middle of the sample, and the random view is the cracks met by chance without any favorite positions.

2 EXPERIMENTAL PROGRAM

The binder consists of cement, fly ash and superplasticizer (SP), and water-to-binder ratio (w/b) is 0.36, where superplasticizer conforming to ASTM C494 Type-G with a specific gravity of 1.1. The total volume fraction of the aggregates is $c_1 = 0.67$ with river sand having a specific gravity of 2.60 and the absorption of 2.5 %, and coarse aggregate is a kind of crushed sandstone with a specific gravity of 2.57 and the absorption of 1.45 %. A mixture proportion of high-performance concrete (HPC) with w/b=0.36 is shown in Table 1, and the slump is 200 ± 30 mm.

Table 1. Mixture proportion of high-performance concrete*.

Water	Cement	Fly ash	Sand	Gravel	SP
160	378	67	730	1020	2.23

*Unit: (kg/m^3)

Material age is of 28 days, and specimen sizes of concrete made by steel molds are of $100\phi \times 200$ mm and $100 \times 100 \times 350$ mm, respectively, to measure the elastic moduli and the fracture toughness. At least six specimens were used to examine the material properties. Specimens were under a uniaxial compression by MTS machine with a constant strain rate $\dot{\varepsilon} = 1 \times 10^{-5}$/sec to measure the longitudinal and lateral strains and plot the stress-strain curves. Fracture toughness was calculated from the three-point bending test.

The crack density of high-performance concrete was determined based on the SEM measurements. The size of SEM specimens is about $3 \times 3 \times 1.5$ mm. The length and the number of microcracks were measured from SEM specimens when the material was under no load, $0.3\, f_c^{'}$ and $0.5\, f_c^{'}$ respectively

in the uniaxial compression test, and was under the fracture strength for the calculations of the fracture toughness, where $f_c^{'}$ is the peak strength of concrete. The observation positions of SEM specimens were at the fixed position and the random one, respectively. Each observation point was viewed by five magnifications: 500×, 1000×, 3000×, 4000× and 5000×.

To evaluate the crack properties, one used Photoshop7.0 software to deal with the SEM picture converted into the monotonic white and black color, and SigmaScan Pro5 software to measure the number and the length of cracks. Besides, the window size of the observation in SEM was also measured. Figure 1 is the SEM picture at a magnification of 4000× while HPC was under the load 0.3 $f_c^{'}$, and Figure 2 is an image transformation of Figure 1 by Photoshop7.0 software.

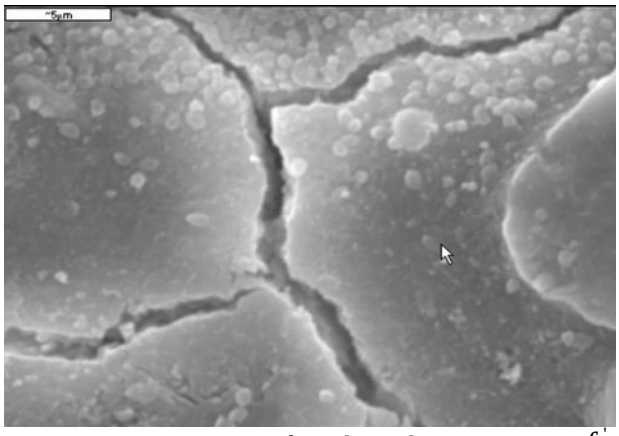

Figure 1. SEM-picture of cracks with 4000× at 0.3 $f_c^{'}$.

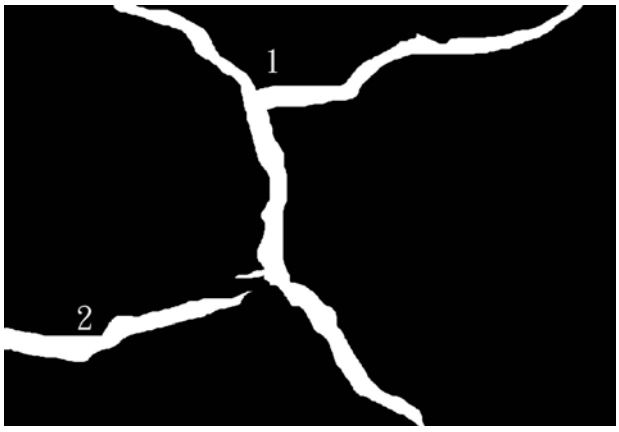

Figure 2. Image transformation of Figure 1 by Photoshop7.0 software.

3 THEORETICAL ANALYSIS

3.1 *Crack density*

Because SEM can only scan a small area of the specimen at a time to view the microcracks, it is difficult to find out the true size and the shape of microcracks and their distributions in the material. That is why one needs to establish some rules to straighten out the meaning of crack density in use, and those rules have to be confirmed correctly.

The definition of crack density parameter, according to Budiansky & O'Connell (1976), is

$$\eta = \frac{2N}{\pi}\left\langle \frac{A^2}{P} \right\rangle \tag{1}$$

where η = crack density, N = total number of cracks per unit volume, A = area of the crack, P = perimeter of the crack, and the angle brackets $<\cdot>$ = volume averaging of the quantity.

To determine the crack density, assuming that the SEM specimens can suitably represent the realistic cracks inside the material, and all cracks are convex and have the same size. Then, a theoretical calculation of the crack density measured from two-dimensional cracks is used as (Budiansky & O'Connell 1976)

$$\eta = \frac{8}{\pi^3} M \cdot \langle l \rangle^2 \tag{2}$$

where $\langle l \rangle$ = average trajectory of the cracks and M = total crack number per unit area in SEM window. Let n, h and w be referred to the crack number, and the height and the width of window, respectively. The total crack number per unit area then is calculated by

$$M = \frac{n}{h \times w} \tag{3}$$

Here, the computation of the crack number n in SEM winder is following the rule that the crack at an obvious turning point is treated as the beginning of a new crack. For example, number 1 crack marked in Figure 2 consists of three cracks in the calculation, where two straight cracks and a bended crack were counted approximately.

3.2 *Effective elastic moduli and fracture toughness*

High-performance concrete is assumed to be a two-phase composite containing concrete without cracks as the matrix and the cracks as the inclusion. Attiogbe (1987) proposed an analytical procedure used to convert two-dimensional crack data into three-dimensional crack distributions in cement paste and mortar, and found that the degree of anisotropy K is about -0.15 when the compressive strain is less 0.002. Thereby, the cracked concrete (composite) as a whole is isotropic if the strain is small.

Pan & Weng (1995) used the inclusion theory (Mori & Tanaka 1973, Weng 1984) to examine the effective elastic bulk modulus κ and effective elastic shear modulus μ of the composite, and concluded that the elastic moduli of isotropic cracked-materials are of less crack-shape sensitivity. Besides, the effective elastic moduli of the material with circular cracks were also found by

$$\frac{\kappa}{\kappa_0} = \frac{1}{1+\frac{16}{9}\frac{1-\nu_0^2}{1-2\nu_0}\eta} \tag{4}$$

$$\frac{\mu}{\mu_0} = \frac{1}{1+\frac{32}{45}\frac{(1-\nu_0)(5-\nu_0)}{2-\nu_0}\eta} \tag{5}$$

where κ_0 = elastic bulk modulus of the matrix (no cracks), μ_0 = elastic shear modulus of the matrix, and ν_0 = Poisson's ratio of the matrix. Due to the less crack-shape sensitivity, one can use Equation 4 and Equation 5 to determine the effective elastic moduli of isotropic HPC containing arbitrary shapes of cracks. The elastic relation still holds for $E = 9\kappa\mu/(3\kappa+\mu)$.

From Equation 4, Equation 5 and the Hooke's law, one can easily find out the relation of Poisson's ratio between the composite (cracked material) and the matrix as

$$\nu = \frac{45(2-\nu_0)\nu_0 + 16\nu_0(1-\nu_0^2)\eta}{45(2-\nu_0)+16(1-\nu_0^2)(10-3\nu_0)\eta} \tag{6}$$

where ν = Poisson's ratio of the cracked material.

Meanwhile, the fracture toughness of the brittle material is usually expressed by the critical stress intensity factor K_c. Let the stress intensity factor of the matrix, the crack-tip stress intensity factor of the composite and the stress intensity factor change (toughness chance) be denoted as K_0, K_{tip} and ΔK, respectively, where the crack-tip stress intensity factor $K_{tip} = K_0 - \Delta K$ and the critical stress intensity factor of the composite $K_c = K_0 + \Delta K$.

Based on a micromechanics approach, the analytic solution of toughness change for a two-phase isotropic composite under Mode I loading has been derived (Pan 1999) and the form is

$$\frac{K_{tip}}{K_0} = f\sqrt{g} \tag{7}$$

where f and g are material parameters. It is noted that, in Equation 7, the ratio K_{tip}/K_0 less than one implies material toughening. From Equation 7 and the relations of K_{tip}, K_0, ΔK and K_c, the stress intensity factor of the material with no cracks has the form as

$$K_0 = \frac{K_c}{2 - f\sqrt{g}} \tag{8}$$

If the cracked material contains circular cracks, the material parameters f and g are

$$f = \frac{27+96k_1(1+\nu_0)^2\eta}{27+4(1+\nu_0)^2\eta} \tag{9}$$

$$g = \frac{45(2-\nu_0)[45(2-\nu_0)+16(1-\nu_0^2)(10-3\nu_0)]}{45(2-\nu_0)^2[45+32(5+\nu_0)\eta]+1024(1-\nu_0^2)(5-\nu_0)(5-2\nu_0)\eta^2} \tag{10}$$

where k_1 = main crack contour factor, and the value $k_1 = 0.072$ for the steady-state propagating crack and $k_1 = 1/24$ for the stationary crack respectively.

Now, in our case, HPC containing microcracks is isotropic. One can use a uniaxial compression and SEM to find the elastic Young modulus, Poisson's ratio and the crack density η of HPC. Of course, the other two elastic moduli κ and μ are also determined from the isotropic relation of HPC.

Once the crack density η and Poisson's ratio ν of the cracked body are known, the Poisson ratio of HPC without cracks (ν_0), calculated from Equation 6, is determined. This Poisson's ratio ν_0 allows us to obtain the elastic bulk modulus κ_0 and shear modulus μ_0 respectively by substituting ν_0 and η into Equation 4 and 5, so as to find Young's modulus E_0 simultaneously. Thereby, the same material subjected to new compressive loads will produce new crack densities, the predicted effective bulk and shear moduli, κ and μ, are found by Equation 4 and 5.

Similarly, from Equation 8, one can calculate the stress intensity factor of the matrix K_0 if the crack density is given. As the material properties of HPC without microcracks are found theoretically, the stress intensity factor increment ΔK due to the microcracking is finally determined by means of Equation 7.

4 RESULTS AND DISCUSSION

4.1 *Representative crack density parameter*

As one knows, different observation magnifications in SEM measurements will lead to different values of crack density in estimations. In this paper, one tries to suggest a representative crack density parameter that can suitably employ to estimate the mechanical properties of cracked cementitious materials.

High-performance concrete with $c_1 = 0.67$ was tested by the uniaxial compression and had the peak stress $f_c' = 48.56$ MPa. SEM with five magnifications from 500× to 5000× and the field at fixed and random position were taken to view the cracks after the designed loading reached, and the results are shown in Figure 3. The estimated crack densities of high-performance concrete at the random position of the view are always greater than those at the fixed position regardless the magnifications, and both values approach to asymptotes as the magnifications increase.

Figure 4 shows the crack densities of concrete in the random view applied to no load, $0.3f_c'$, $0.5f_c'$ and f_c', respectively. Those crack densities also tend to some asymptotic constants when the magni-

fications are greater than 3000×. From Figure 3 and Figure 4, it seems that the estimated crack density may be insensitive to the magnifications and the observation positions if the magnifications are of 3000 × or larger, and this range of crack density might be chosen as the representative crack density parameter which we can use to evaluate the material properties. However, it is still needed to inspect carefully.

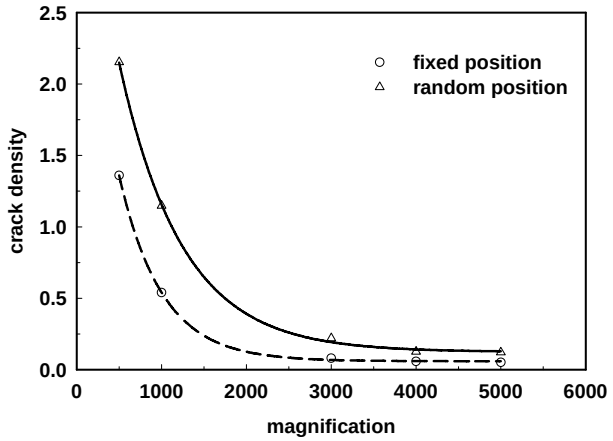

Figure 3. Crack density of different views after failure.

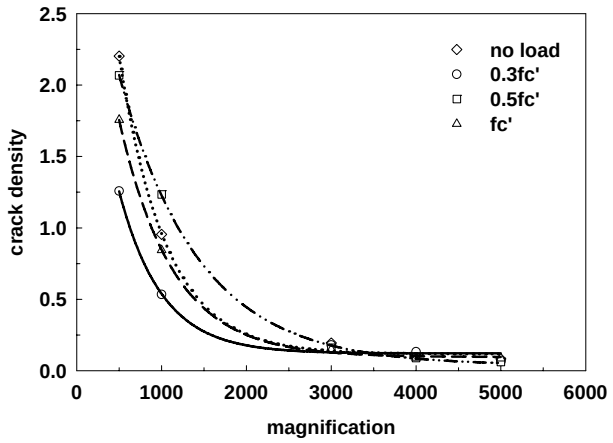

Figure 4. Crack density of random position with different loads.

Although different SEM magnifications will lead to different crack densities in calculations, the properties of cracked material are unique in experiments. To examine the effect of the magnification, average crack densities calculated from two groups of 500× ~ 5000× and 3000× ~ 5000× were chosen to estimate the elastic moduli of the material without cracks.

The elastic moduli of high-performance concrete with $c_1 = 0.67$ subjected to a uniaxial compression $0.52\ f_c^{'}$ are shown in Table 2. Those experimental data allow us to theoretically find the elastic moduli of material containing no cracks (matrix). For example, the experimental crack densities at the magnification range of 3000× ~ 5000× in fixed view and random view are $\eta = 0.123$ and $\eta = 0.146$, respectively, and then from Equation 6 the Poisson ratio of concrete without cracks ν_0 is found to be 0.289 and 0.297 in turns.

Table 2. Elastic moduli under $0.52\ f_c^{'}$.

E（GPa）	ν	μ（GPa）	κ（GPa）
21.39	0.244	8.60	13.92

From Table 2 and Equations 4-10, the calculated results for the shear modulus, bulk modulus and fracture toughness of the matrix (no cracks exist) are shown in Table 3, and their statistical variances are also shown in Table 4. In Table 3, the differences of average material properties at the magnification range of 500× ~ 5000× are pretty large in both fixed view and random view. In Table 4, the variances of elastic moduli and fracture toughness at the magnification range of 3000× ~ 5000× are far less than those of 500× ~ 5000×. Therefore, the crack density at the magnification range of 3000× ~ 5000× is suitable for selecting as the representative crack density parameter in concrete.

Table 3. Average properties of the matrix.

Properties	Observation	Magnification	
		500x~5000x	3000x~5000x
μ_0 (GPa)	Fixed	14.61	10.07
	Random	18.79	10.33
κ_0 (GPa)	Fixed	40.97	20.56
	Random	61.69	22.06
K_0	Fixed	0.615	0.774
($MPa\sqrt{m}$)	Random	0.581	0.695

Table 4. Variance of average properties of the matrix.

Properties	Observation	Magnification	
		500x~5000x	3000x~5000x
μ_0 (GPa)	Fixed	661.02	3.67
	Random	3575.78	15.01
κ_0 (GPa)	Fixed	0.048	0.017
	Random	0.028	0.014
K_0	Fixed	661.02	3.67
($MPa\sqrt{m}$)	Random	3575.78	15.01

4.2 *Theoretical verification*

Now the representative crack density parameter η is selected at the magnification range of 3000× ~ 5000× in use. This representative crack density parameter (RCDP) is considered as an important factor to evaluate the mechanical properties of cracked material. Here, the elastic moduli and fracture toughness of the matrix in Table 3 at the range of 3000× ~ 5000× are taken to estimate the effective bulk and shear moduli, and fracture toughness of high-performance concrete containing the aggregate $c_1 = 0.67$.

Based on the material properties of the matrix in Table 3 and the representative crack density parame-

ters measured from HPC subjected to no load, 0.3 $f_c^{'}$ and 0.5 $f_c^{'}$ respectively, the experimental values and theoretical calculations for the effective bulk and shear moduli are shown in Table 5. The predicted effective bulk and shear modulus at fixed view are close to those at random view regardless of the applied stress. It means that one can use the SEM observation either at fixed view or at random view to measure the crack properties if the magnification is of 3000× ~ 5000×.

Table 5. Comparisons of effective elastic moduli.

Properties	Observation	No load	0.3 $f_c^{'}$	0.5 $f_c^{'}$
μ (GPa)	Experiment	8.66	7.74	7.37
	Fixed	9.27	9.01	8.65
	Random	9.09	8.82	8.68
κ (GPa)	Experiment	14.03	12.53	11.93
	Fixed	16.59	15.48	14.13
	Random	15.81	14.76	14.22
η	Fixed	0.062	0.085	0.118
	Random	0.099	0.124	0.138

Compared with the experimental data in Table 5, the predicted effective elastic bulk and shear moduli have the errors from 5% to 18% approximately. Table 6 shows the fracture toughness for experimental data and the predictions. The predicted fracture toughness is in an acceptable range as compared with the experimental data in Table 6.

Table 6. Comparisons of fracture toughness.

Properties	Experiment	Fixed	Random
$K_c\,(MPa\sqrt{m})$	0.512	0.550	0.542
η	---	0.238	0.149

Finally, the effective Young modulus of high-performance concrete subjected to different loads is calculated with five magnifications, and the results are shown in Table 7 and Figures 5-6. By comparing with the experimental data, the predicted results calculated from the crack density at 500× and 1000× are not acceptable shown in Figures 5-6. Let the stress-strain relations in Figures 5-6 be enlarged near the experimental curves and re-plotted in Figures 7-8, obviously, the predicted effective Young modulus calculated from the magnification of 3000× is close to the experimental data. Hence, the better choice for representative crack density parameter is the cracks measured at the magnification near 3000×.

Table 7. Comparisons of effective Young modulus (GPa).

Observation	Magnification	No load	0.3 $f_c^{'}$	0.5 $f_c^{'}$
Experiment		21.55	19.25	18.33
Fixed	500x	5.87	6.18	8.243
	1000x	10.49	11.32	10.63
	3000x	22.81	21.09	20.13
	4000x	23.62	23.46	21.97
	5000x	23.89	23.54	22.70
Random	500x	5.13	12.37	4.45
	1000x	9.44	17.21	12.73
	3000x	21.22	20.07	19.41
	4000x	22.75	22.36	22.01
	5000x	24.96	24.18	23.99

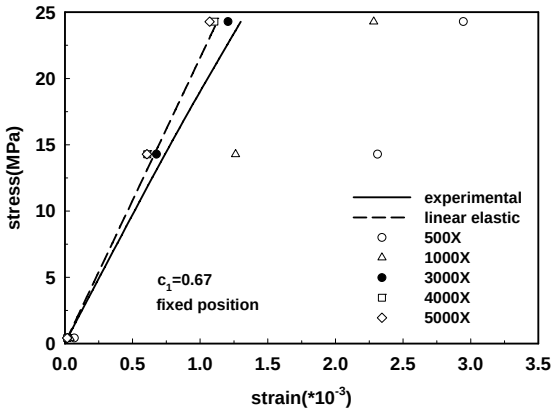

Figure 5. Stress-strain curves at fixed view.

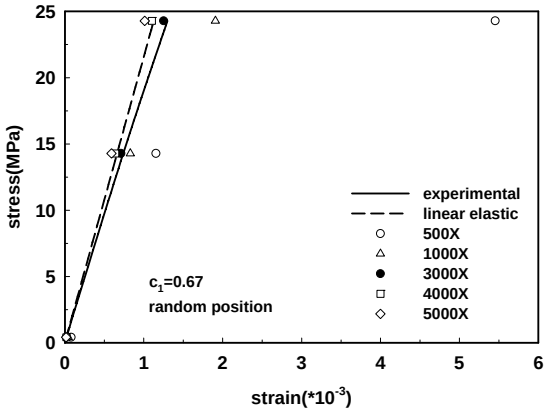

Figure 6. Stress-strain curves at random view.

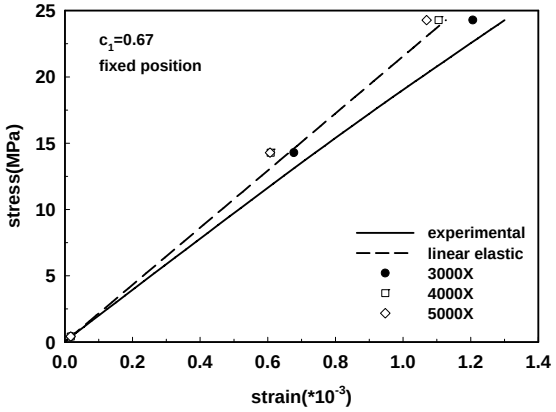

Figure 7. Enlarged stress-strain curves at fixed view.

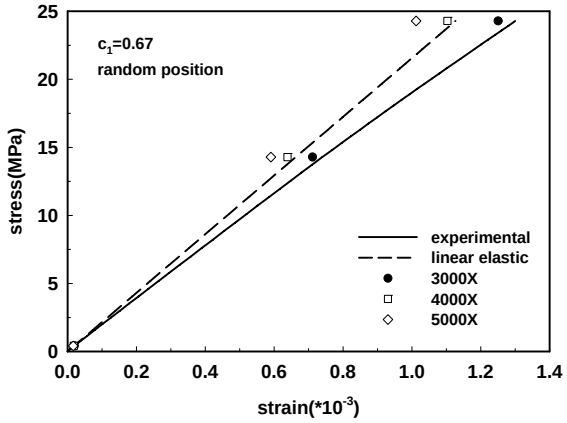

Figure 8. Enlarged stress-strain curves at random view.

5 CONCLUDING REMARKS

Based on SEM measurements and the verification of the micromechanics approach, the estimated crack density at the magnification range of 3000× ~ 5000× can be considered as the representative crack density parameter in concrete or cementitious materials. This representative crack density parameter allows us to determine the mechanical properties of cracked cementitious material if the microcracks are randomly oriented. For high-performance concrete with the volume fraction of the aggregates $c_1 = 0.67$, the representative crack density is better observed around the magnification of 3000×.

ACKNOWLEDGMENT

The funding of this research was partially supported by the Taiwan National Science Council under Grant NSC 95-2221-E-151-046.

REFERENCES

Attiogbe, E. K. & Darwin, D. 1986. Correction of window size distortion of crack distributions on plane sections. *J. of Microscopy* 114(1): 71-82.

Attiogbe, E. K. & Darwin, D. 1987. Submicrocracking in cement paste and mortar. *ACI Journal* 84-M43: 491-500.

Budiansky, B. & O'Connell, R. J. 1976. Elastic moduli of a crack solid. *Int. J. Solids Structures* 12: 81-97.

Erick, R. 1988. Automatic quantification of microcracks network by stereological method of total projections in mortars and concretes. *C.C.R.* 18: 35-43.

Mori, T. & Tanaka, K. 1973. Average stress in the matrix and average elastic energy of materials with misfitting inclusions. *Acta Metall.* 21: 571-574.

Oillivier, J. P. 1985. A non destructive procedure to observe the microcracks of concrete by scanning electron microscopy. *C.C.R.* 15(3): 1055-1060.

Pan H. H. & Weng, G. J. 1995. Elastic moduli of heterogeneous solids with ellipsoidal inclusions and elliptic cracks. *Acta Mechanica* 110: 73-94.

Pan H. H. 1999. An overall approach for microcrack and inhomogeneity toughening in brittle solids. *Chinese J. Mechanics* 15(2): 57-68.

Weng, G. J. 1984. Some elastic properties of reinforced solids, with special reference to isotropic ones containing spherical inclusion. *Int. J. Engng. Sci.* 22: 845-856.